Long-Range Electron Transport of Ruthenium-Centered Multilayer Films *via* a Stepping-Stone Mechanism

Kei-ichi Terada,[†,∥] Hisao Nakamura,[‡] Katsuhiko Kanaizuka,[§,⊥] Masa-aki Haga,[§] Yoshihiro Asai,[‡,*] and Takao Ishida[†,*]

[†]Nanosystem Research Institute (NRI), National Institute of Advanced Industrial Science and Technology (AIST), 1-2-1 Namiki, Tsukuba, Ibaraki 305-8564, Japan, [‡]Nanosystem Research Institute (NRI), "RICS", AIST, 1-1-1 Umezono, Tsukuba, Ibaraki 305-8568, Japan, [§]Department of Applied Chemistry, Faculty of Science and Engineering, Chuo University, 1-13-27 Kasuga, Bunkyo-ku, Tokyo 112-8551, Japan, and [⊥]Department of Material and Biological Chemistry, Faculty of Science, Yamagata University, 1-4-12 Kozirakawa-machi, Yamagata, 990-8560, Japan. [∥]Present address: KST World Corp., Fukui, Japan.

ABSTRACT

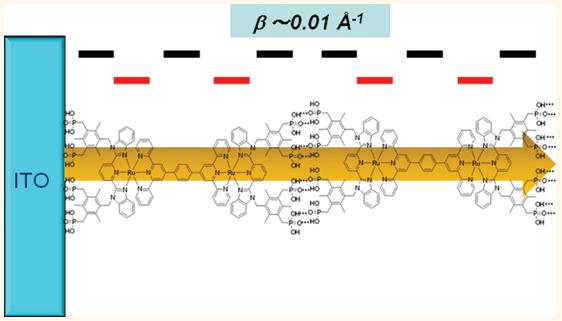

We studied electron transport of Ru complex multilayer films, whose structure resembles redox-active complex films known in the literature to have long-range electron transport abilities. Hydrogen bond formation in terms of pH control was used to induce spontaneous growth of a Ru complex multilayer. We made a cross-check between electrochemical measurements and *I*—*V* measurements using PEDOT:PSS to eliminate the risk of pinhole contributions to the mechanism and have found small β values of 0.012—0.021 Å^{-1}. Our Ru complex layers exhibit long-range electron transport but with low conductance. On the basis of the results of our theoretical—experimental collaboration, we propose a modified tunneling mechanism named the "stepping-stone mechanism", where the alignment of site potentials forms a narrow band around E_F, making resonant tunneling possible. Our observations may support Tuccito *et al.*'s proposed mechanism.

KEYWORDS: molecular electronics · metal complex · self-assembly · electron transport · stepping stone

The future of molecular devices (molecular electronics) may be successful[1] if the following problems with molecular junctions can be resolved: (i) a lack of mechanical robustness and (ii) the exponential decay of thickness (*L*) dependence of the charge migration rate, *i.e.*, $\propto e^{-\beta L}$,[2−4] where β is the slope of the exponential decay. Here, we use the term "charge migration" to represent both conductance and electron transfer rate. There have been several past attempts to create mechanically stable single-molecular junctions.[5,6] If we were able to make self-assembled mono/multilayers (SAMs) where independent single-molecular conduction is dominant, the problem might become easier to solve. One of the key factors to make this possible is the use of multileg molecules such as tripod molecules.

Issue (ii) needs to be carefully addressed in designing molecular devices. If the electronic energy level of the bridge molecule is aligned with the Fermi energy (E_F), resonant tunneling predominates. In this resonant tunneling mechanism, the exponent β becomes 0 due to the perfect transmission.[7] Electron transport through metal atomic wire corresponds to this case. On the other hand, organic molecules usually have a large energy gap between the highest occupied molecular orbital (HOMO) and lowest unoccupied molecular orbital (LUMO), both of which are located far from E_F; thus, the tunneling is *off-resonant:* exponential decay of the length dependence of the charge migration rate is fairly common in organic molecules.[3,4,7] In this case, the β value becomes larger if the HOMO/LUMO gap of the bridging molecule increases. The charge migration mechanism dominated by off-resonant tunneling is often called the superexchange mechanism.[2] Thus, organic molecules are not ideal in light of criterion (ii). However, some reports suggest that organometallic molecules may not behave similarly to organic molecules.

In the 1990s, Hong and Mallouk made a series of electron transfer rate measurements of molecular films with various thickness of the spacer layer.[8,9] A multilayer film

* Address correspondence to yo-asai@aist.go.jp; t-ishida@aist.go.jp.

Received for review July 26, 2011 and accepted February 11, 2012.

Published online February 11, 2012
10.1021/nn300126m

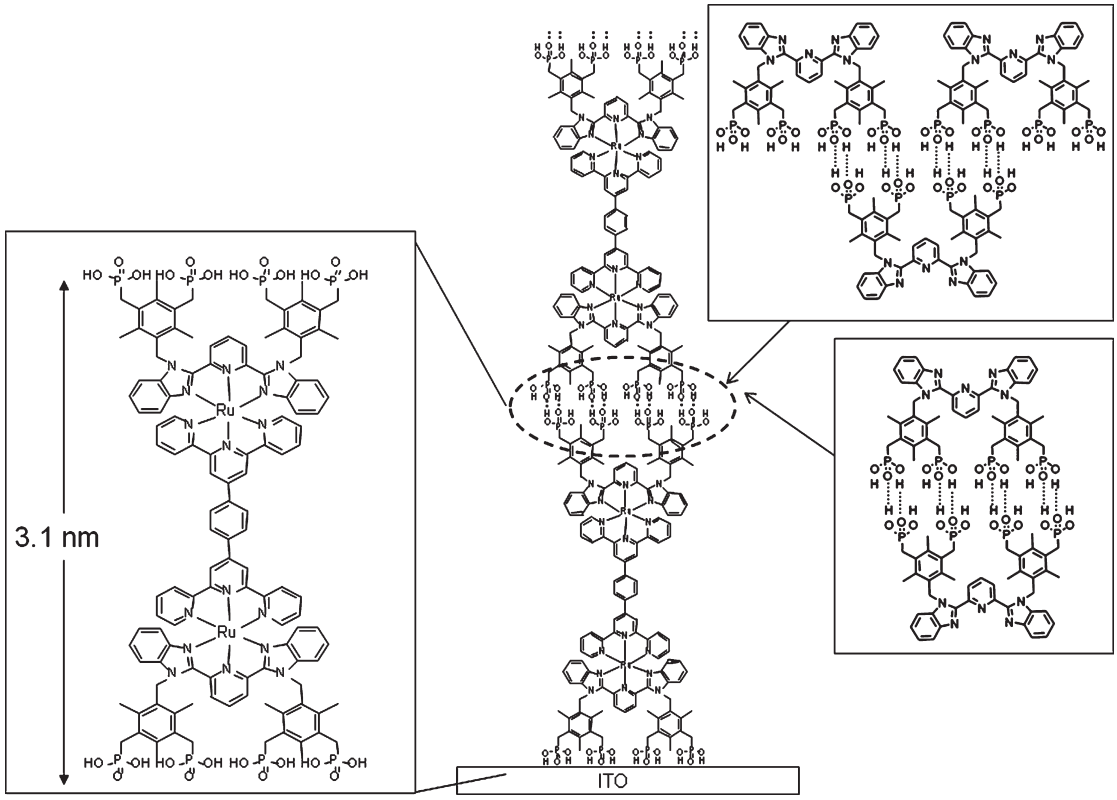

Figure 1. Schematic drawing of the multilayer structure of our Ru complex designed to have multileg anchoring onto the ITO substrate *via* the hydrogen bonds of the phosphonic acid groups.[14,15] Two possible multiple-hydrogen-bonding interactions between phosphonic acids are shown in the boxed columns.

was prepared sequentially, and they estimated its β value in terms of electrochemical measurements. The unit layer of the film includes a metal atom (zirconium) phosphonate. Although zirconium phosphonate is an unconjugated insulator, the observed β value was much smaller than the value predicted for conjugated oligomers.[8] Possible reasons were discussed, *e.g.*, charge diffusion through defects in the film, pinhole effects related to diffusion of electroactive species, and heterogeneity (disorder) of the active site.[10] They excluded the possibility of direct tunneling through the organic molecular layer.

Tuccito *et al.* recently found that organometallic layers give very small β values through a series of electronic current measurements using Hg drop electrodes.[11] The β values for a molecular wire of bis(terpyridine)iron and bis(terpyridine)cobalt complex were estimated to be 0.028 and 0.001 $Å^{-1}$, respectively. In their experiments, the carbon backbones (cages) were assembled to provide well-controlled orientation of the phenyl rings, while the metal centers were incorporated in a stepwise manner. The wire was anchored to electrodes by a thiol (*i.e.*, a SAM junction) rather than the spacer-acceptor (redox species) structure described in ref 8. They suggested a direct tunneling mechanism based on experimental observation of the linear dependence of the electric current on $1/N$, where N is the number of metal centers. Because electronic energy levels of organic molecules may stray from E_F, a very small β value cannot be explained by the standard off-resonant tunneling mechanism. They suggested a possibility that the resonance may be mediated by metal centers without discussing details. It should be noted that simple resonance would be accompanied by high conductance. Another mechanism based on thermally induced hopping (TIH)[2] has been discussed for the redox-active center complex.[2,12,13] In this case, the current should be linearly dependent on $1/N^2$ (or a higher order) rather than on $1/N$. This does not agree with the results given in ref 11, as discussed above. Furthermore, the current should exhibit activation-type temperature dependence in the case of the TIH mechanism.

In the present study, we will discuss the mechanism of the small β problem both experimentally and theoretically, focusing on the special role of the metal centers, to explain long-range electron transport through the metal complex layer. We made a cross-check between electrochemical measurements and $I-V$ measurements using PEDOT:PSS in sandwiched solid cells to reduce the possibility of pinhole contribution to the charge migration mechanism. On the basis of the experimental results followed by our theoretical–experimental collaboration, we propose a novel tunneling mechanism that we named the "stepping-stone

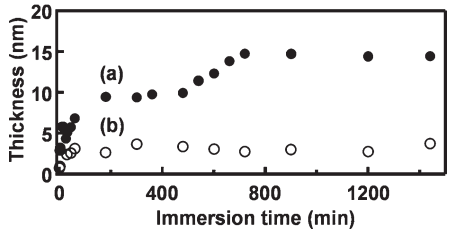

Figure 2. Immersion time dependence of the Ru complex layer thickness estimated using XPS data. The thicknesses of the Ru complex layers immobilized on ITO were calculated using the equation $d = -\lambda \cos\theta \ln(I/I_0)$,[17] where d is the film thickness, I_0 and I are the In(3d) intensity before and after film formation, λ is the attenuation length of the In(3d) electron from the ITO surface, and θ is the takeoff angle from the surface normal. In the present study, we measured the spectrum at $\theta = 0$. We used a wavelength (λ) of 3.5 nm to determine the thickness of the Ru complex layer.[17] Black (a) and white (b) circles respectively denote the data obtained when we used pH 3 and pH 6 solutions.

mechanism". By applying first-principles calculations and theoretical analysis to the experimental results, we obtained some support for this mechanism.

RESULTS AND DISCUSSION

Sample Preparation. We have prepared supramolecular assemblies based on our design for the redox-active Ru complex with phosphonate anchoring groups to fabricate a nanofunctional layered architecture on a solid surface.[14,15] We fabricated a multilayer film using the Ru complex with the Zr(IV) ion acting as a chemical glue in successive immersion processes, which is basically the same technique as that adopted by Hong and Mallouk.[8,9] In addition to this, we have used the fact that molecules with phosphonic acids can form multilayer films in one step when low-pH solution is used. This is because hydrogen bonds between phosphonic acids are formed under low-pH conditions (Figure 1). Because of the similarities between our film and that of Tuccito *et al.*,[11] we anticipate that our Ru complex multilayer film might exhibit long-range electron transport ability similar to their observations. We have demonstrated this experimentally. To our surprise, the molecular film has fair conduction, even though phosphonic acid groups form a large potential barrier against the charge migration. This spawned another subject for theory. In this paper, we discuss the details of the mechanism both theoretically and experimentally, including this problem.

Film Thickness Measurements of the Ru Complex. Prior to discussing transport measurements, we elucidate how we monitored multilayer film formation of the Ru complex assemblies. This was done by means of X-ray photoelectron spectroscopy (XPS), Fourier transform infrared spectroscopy (FT-IR), atomic force microscopy (AFM), and electrochemical methods. Spontaneous multilayer formation of a metal complex on an ITO surface has been reported.[16] We estimated the thicknesses of the Ru complex layers using XPS[17] as a function of the immersion time in pH 3 solution (Figure 2). The thicknesses of the molecular layer films made by immersion for 30 min, 1 h, 5 h, 10 h, and 20 h were estimated experimentally to be 3.2, 6.8, 9.4, 12.3, and 14.4 nm, respectively. Since the DFT calculation suggested the molecular length of the Ru complex monolayer to be $\sim 3.1 \pm 0.2$ nm, these thicknesses may be attributable to the mono-, bi-, three, four, and five layers of the Ru complex. We found that a different pH value (pH 6) is ineffective (*cf.* Figure 2b). In some particular cases, we measured glancing-angle X-ray diffraction. The thicknesses of the molecular layer films prepared by immersion for 8 and 24 h were estimated to be 7.3 and 18.7 nm, respectively.

TABLE 1. Root-Mean-Square (rms) and the Least Thickness Values of the Ru Complex Layers[a]

immersion time	rms (nm)	the least thickness (nm)
30 min (monolayer)	0.52	1.7
1 h (bilayer)	0.79	4.6
5 h (3 layers)	1.68	6.6
10 h (4 layers)	1.06	9.0
20 h (5 layers)	1.57	10.4

[a] The definition and the method of how we estimate the least thickness is described in the text.

We confirmed formation of hydrogen bonds by FT-IR. In the FT-IR spectra of the Ru complex layers (Figure S1 in the Supporting Information), a broad peak assigned to the P═O vibration mode was observed between 1150 and 1350 cm^{-1}. Since similar broadening of the P═O vibration mode was reported in the case of phosphonate adsorption on the TiO_2 surface,[18] we believe that the broadening of the peaks between 1150 and 1350 cm^{-1} proves the formation of the hydrogen bonds between the Ru complex layers. The surface roughness for each layer number was also evaluated by AFM. The root-mean-square (rms) values of mono-, bi-, three, four, and five layers of the Ru complex layer were 0.52, 0.79, 1.68, 1.06, and 1.57 nm, respectively (Table 1). The height profile given in Figure S2 of the Supporting Information tells us that the maximum variance of the film thickness is estimated to be about 3 nm when the immersion time is more than 30 min. It should be noted that the average film thickness is measured by XPS, and it corresponds to the half-height of the vertical axis of the height profile box given in Figure S2. We may have to take into account the roughness effect expressed in terms of the height variance to avoid overestimation of the β value. In this paper, we evaluate the β value using the worst scenario, where the electron current pathway is given by the through-bond path with the least thickness. The least thickness is estimated by using the lowest position denoted by "0" of the height profile. Our estimate will give an upper bound β value. The least thicknesses of mono-, bi-, three, four, and five layers of the Ru

complex are estimated to be 1.7, 4.6, 6.6, 9.0, and 10.4 nm, respectively (see Table 1).

Using cyclic voltammgrams (CVs) measured in CH_3CN containing 0.1 M TBAP (*cf.* Figure S3 in the Supporting Information), we estimated the coverage values of Ru complex layers (Table 2). The average surface coverage values of mono-, bi-, three, four, and five layers were estimated. The Γ value increases almost linearly as a function of the number of Ru complex layers: this is in good agreement with the XPS data.

***β* Value Measurements.** So far, β values through the molecular layer have been estimated in the literature by using several methods, including electrochemistry (chronoamperometry),[8,13,16,19] scanning tunneling microscopy,[20] conducting probe AFM (CP-AFM),[21−24] and Hg drop junctions.[11,25,26] Concerns have occasionally been raised about the bulk measurement methods such as the electrochemical method because of the risk of pinhole effects.[8−10,16] To obtain an accurate β value for the direct tunneling process, the pinhole and the heterogeneity effects need to be minimized. Because of this, Akkerman *et al.* used a top electrode made of conducting polymer in their sandwiched solid cell.[27−29] Poly(3,4-ethylenedioxythiophene) stabilized with poly(4-styrenesulfonic acids) (hereafter PEDOT:PSS) was adopted because the dominant size of PEDOT:PSS (∼20−30 nm) is sufficiently large to prevent penetration into the molecular layer as well as into nanosized pinholes.[29] We have compared the results of both the electrochemical method and the method using a sandwiched solid cell, which has a lower risk of pinholes. Using this method, we avoid confusion such as that caused by pinholes.

TABLE 2. Average Surface Coverage Values (Γ) of Ru Complex Layers, Estimated Using CVs

immersion time	Γ (mol cm^{-2})
30 min (monolayer)	$(5.3 \pm 0.3) \times 10^{-11}$
1 h (bilayer)	$(8.6 \pm 1.4) \times 10^{-11}$
5 h (3 layers)	$(2.1 \pm 0.5) \times 10^{-10}$
10 h (4 layers)	$(3.1 \pm 0.5) \times 10^{-10}$
20 h (5 layers)	$(4.1 \pm 0.4) \times 10^{-10}$

The data measured with chronoampermetry for the Ru complex layers on ITO substrates are summarized in Figure 3. Figure 3a shows the transitional anodic current curves of the Ru complex layers with a potential step from +0.4 V to +1.17 V to cross over the redox potential of Ru complex layers at approximately +0.70 V *vs* Ag/Ag^+. The relation between the transitional current I_c and transfer constant k_{app} is expressed as a function of time t, $\ln|I_c(t)/I_c(0)| = -k_{app}t$. In Figure 3b, the slope of $\ln I_c$ *vs* time is shown. As stated above, exponential decay of k_{app} as a function of distance is expected in normal organic systems.[8,11−13,20−26] The β value was then estimated to be 0.021 Å^{-1} (Figure 3c).

Figure 4 shows a schematic drawing of the cell structure, $I-V$ curves of the PEDOT:PSS|Ru complex layer|ITO sandwiched junction, and log(I) as a function of average thickness. Before formation of the Ru complex layer onto the ITO surface, a polycrystalline insulating TiO_2 layer (∼100 nm) was deposited onto the ITO substrate covered by a metal mask using rf-magnetron sputtering. After the immobilization of the Ru complex layer, a 4 μm PEDOT:PSS film was coated on the Ru complex layer to create the top electrode. To increase the conduction of the PEDOT:PSS film, a small amount of ethylene glycol was added to the PEDOT:PSS liquid.[30] The experimental details are described in a later section.

For the monolayer, bilayer, and three layers, the $I-V$ curves are almost symmetric (*cf.* Figure 4b). At more than four layers, the $I-V$ curves often become asymmetric. The observed electric current at a lower voltage (>−200 and <+200 mV) decreases exponentially as a function of the thickness. By making a linear fit of the curve, the β values at +200 and −200 mV were estimated to be 0.015 and 0.012 Å^{-1}, respectively (Figure 4c). The estimated β values here are close to

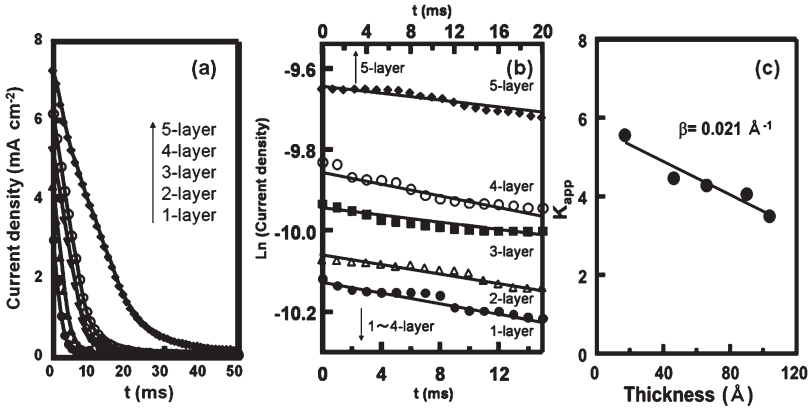

Figure 3. (a) Current (I_c)−time (t) plots of Ru complex layers; (b) log−linear plots of (a); (c) film thickness dependence of log(k_{app}), where k_{app} is the apparent electron transfer constant through the multilayer film. The measurements were done in 0.1 M TBAP CH_3CN solution.

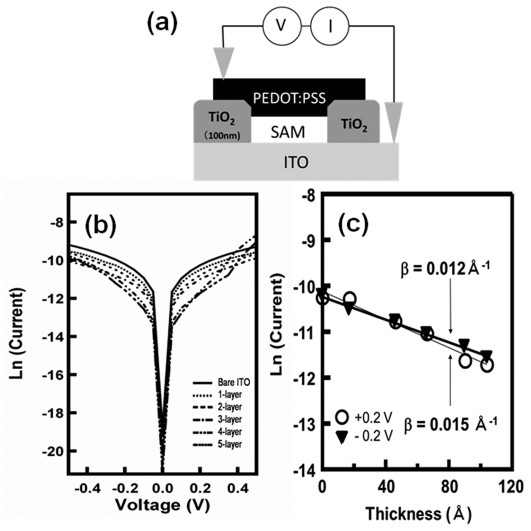

Figure 4. (a) Schematic drawing of solid-state cell of PEDOT:PSS|Ru complex layer| ITO junction; (b) current (I_c)−voltage (V) plots of PEDOT:PSS Ru complex layer ITO junctions; (c) Ru complex layer thickness dependence of log(I_c).

TABLE 3. Activation Energies of Electron Transport, Estimated Using Sandwiched Cells

	activation energy (meV)	
no. of layers	<200 K	>200 K
monolayer	10	390
3 layers	16	83
5 layers	10	36

those estimated from chronoamperometry. A similar tendency of the β values has already been reported in the case of redox-active metal complex layers.[11,13]

In our solid-state measurements using a conductive polymer electrode, the density of the direct contact area of the conducting polymer on the ITO surface is likely to be low, as mentioned previously. Thus, we believe that the low β value comes from the Ru complex layers. As noted above, we notice that surface roughness could influence the apparent β values. In such a case, the real thickness may be lower than that estimated using XPS. Then, in estimating the β value, we suppose that the electron current pathway is given by a through-bond path with the least thickness to avoid overestimation. For comparison, we made sandwiched cells of PEDOT:PSS|insulating alkyl phosphonic acid (C8 and C18) SAM|ITO and obtained a β value of 0.58 Å^{-1}. The β value of sandwiched cells of insulating alkyl phosphonic acids is comparable to those previously reported for the alkyl chain (0.5−1.3 Å^{-1}).[20,21] This may support the assertion that the β value obtained is intrinsic. We occasionally measured the activation energies for charge migration (*cf.* Table 3 and Figure S4, Supporting Information). The activation energy values estimated at low temperature (<200 K) are within the range 10−16 meV. Thus, charge migration is less temperature-dependent. This favors the direct tunneling.

Some groups have reported small β values for redox complexes. These were estimated from electrical conductivity measurements in a dry state or from wet electrochemical measurements. The values obtained are within the range 0.001−0.07 Å^{-1}.[11,13,16,19] The conductance magnitudes in the literature are somewhat lower (observed tunneling resistances are on the order of 1×10^{11} Ω). In our case, the β values and the resistance were 0.012−0.021 Å^{-1} and on the order of 10^9−10^{11} Ω, respectively, demonstrating that low conductivity and long-range transport ability may coexist. The origin of this feature will be discussed in subsequent sections.

Theoretical Background of Electron Transport. Electron transfer through the redox-active molecular layers was assumed to be mediated by redox centers.[11] While the origin of the small β value in organometallic complexes has not yet been fully understood, we assume that direct tunneling is of primary importance. We will continue with these ideas, discussing a possible mechanism with a microscopic approach based on a tight binding model and first-principles calculations.

The conductance G_F and the rate k_{app} are given in terms of transmission coefficient $T(E) = \Gamma_L\Gamma_R|G_{1N}(E)|^2$ by $G_F = (e^2/(\pi\hbar))T(E_F)$ and $k_{app} = ((2\pi)/\hbar)\Gamma_L\Gamma_R|G_{1N}(E_{DA})|^2$-(FC), where G_{1N} is the terminal Green's function of the electron.[3,4,7,31] The constant $e^2/(\pi\hbar)$ is the unit conductance, where e is an elementary charge and $\hbar$ is Plank's constant. E_{DA} is the energy of the donor and the acceptor, while E_F is the Fermi energy of the electrodes. The term $\Gamma_L(R)$ denotes coupling between the molecule and left (right) electrodes (the donor/acceptor), and the term (FC) is the Franck−Condon factor. The terminal Green's function $G_{1N}(E)$ and subsequent $T(E)$ include all the length-dependent information on the conductance and the rate. Here, we briefly discuss the theoretical relationship between the electron transfer and electric conducting systems. While chemical situations are largely different, *i.e.*, charge carrier donation and accepting take place both at the contact between the molecule and at the electrode in the latter system, whereas in the former system one of these happens at the interface between solution and the molecule, the two systems have a common mathematical feature because of the relation $k_{app} = ((2\pi)/\hbar)T(E_{DA})$(FC). Therefore, understanding length dependence of the former leads to that of the latter, provided that direct tunneling such as a superexchange mechanism predominates.

The length dependence of the transmission coefficient of a uniform chain has been discussed in terms of a single-band tight binding model.[7] A brief review is given as follows. One of the most important results is that the length dependence changes from exponential

decay behavior (with the exponent β) to oscillating behavior (with $\beta = 0$) as we move from the off-resonant to the resonant regime. Here, the criteria for the two regimes are determined by E_F or E_{DA}. When they fall within the range of the bandwidth ($2t$) centered at the atomic potential energy (e), the tunneling is resonant and $\beta = 0$. In the off-resonant tunneling region

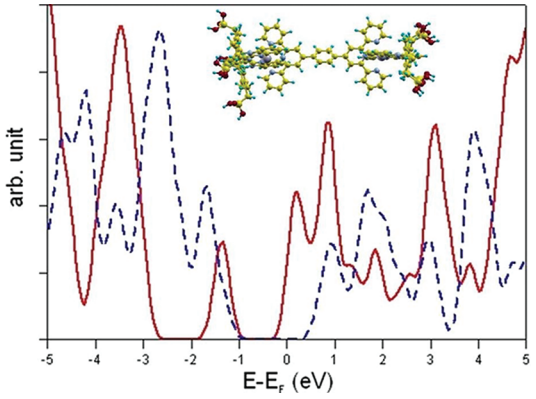

Figure 5. Calculated equilibrium structure and electronic density of state (DOS) of the unit layer of the Ru complex given in Figure 1. The origin of the energy axis is given by the Fermi level E_F of the layer. The solid red line represents the DOS of the layer, and the broken blue line denotes the DOS of the vacancy system. The largest two spheres represent two Ru atoms; each is coordinated by six N atoms. The complex is terminated by phosphoric acid on the left/right sides, which have a P atom and four O atoms at each contact point. The smallest spheres represent H atoms, while the second smallest spheres denote C atoms.

(*i.e.*, $|e - E_F| > 2t$), the exponent β is provided by $\beta = 2 \log(|(e - E_F)/t|)$, and its lower bound β_{LB} is given by 2 log 2. (See Figures 3 and 4 in ref 7.) In addition, $T(E_F)$ reaches 1 periodically in the resonant tunneling regime: that is, it oscillates as periodic function of the length with maximum of 1.

There are two physical conditions that change the results described above. The first one is vibronic coupling. Here, we assume that vibronic coupling is weak. Note that a strong coupling limit gives the TIH,[32] which is out the scope of the present study. If vibronic coupling is sufficiently weak, its effect may be represented by the dephasing constant κ. The oscillation of the transmission coefficient is now damped oscillation, and its exponent γ is expressed as $\gamma = \ln(1 + |\kappa/t|)$, *i.e.*, independent of the gap $|e - E_F|$.[7] Hence, the slope of the exponential decay is determined wholly by the vibronic coupling γ (not by β) in the resonant tunneling regime of the uniform chain model.

Another physical condition is "contact asymmetry". In this case, the coupling strength of the organometallic complex to the left and right electrodes (donor and acceptor) may be very different, *i.e.*, $|\Gamma_L/\Gamma_R| \ll 1$ or $1 \ll |\Gamma_L/\Gamma_R|$. Unlike in symmetric contact, the maximum conductance value is markedly reduced by contact asymmetry. As a result, a low charge migration rate (*i.e.*, $T(E_F) \ll 1$) is possible, even when the resonant condition is satisfied. This is well-known theoretically.[33] See, for example, page 14 of ref 33.

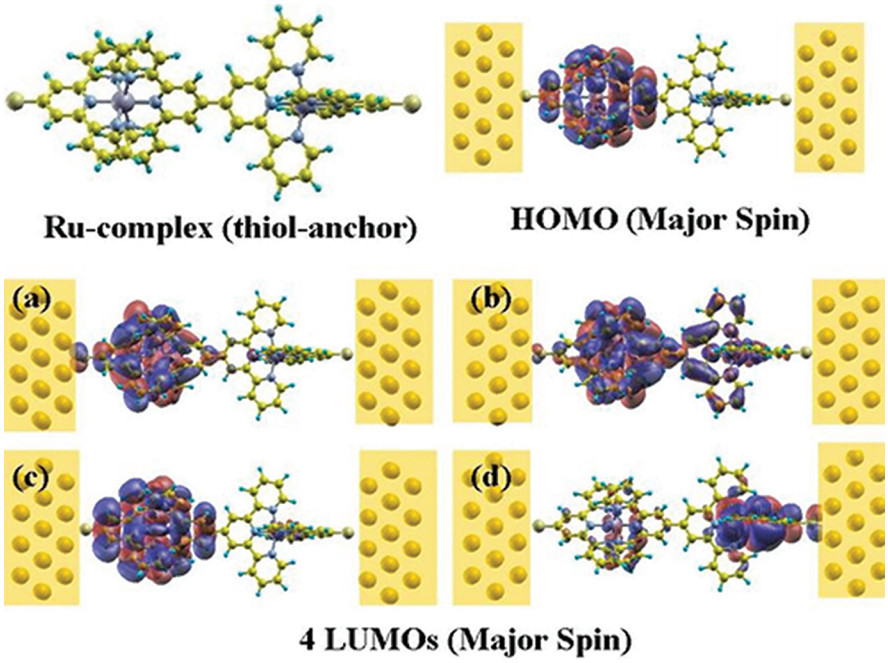

Figure 6. Model Ru complex (left upper panel). First, Au(001) was used instead of ITO as the electrodes. The multileg phosphoric acid anchors were replaced by a thiol anchor. The notations of the spheres are the same as in Figure 5, while the complex is terminated by an S atom instead of phosphoric acid. The projected molecular orbitals (PMO) onto the Ru complex around E_F of the gold electrodes are also shown (right upper, middle, and bottom panels). Red and blue respectively indicate positive and negative amplitudes of the molecular orbital. Yellow denotes the electrodes. The left and the right overlap between the complex and electrodes are largely asymmetric. (See text.)

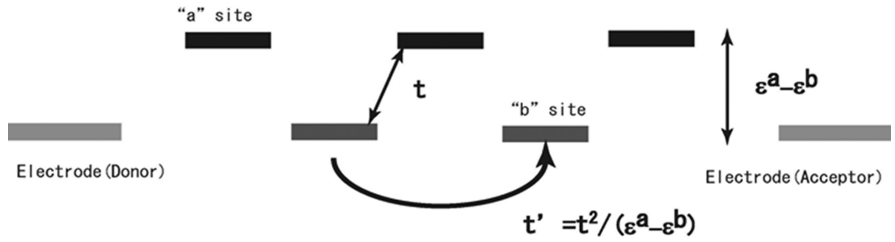

Figure 7. Drawings representing potential alignment in the molecular Hamiltonian, H_{mol}, for an organometallic complex molecular chain (case (ii)). Direct transfer of electrons between two adjacent "*b*" sites with transfer integral t' arises in terms of the second-order process drawn here, causing the formation of a density close to ε^b with bandwidth $2t'$. If *b* is made of the same atomic element as the electrode (donor/acceptor), we may expect ε^b to be resonant with E_F and/or E_{DA}.

First-Principles Calculations. Before we build a model to analyze the mechanism of the small β value as well as the role of metal centers, it would be useful to discuss some first-principles electronic structure calculation results. We began by searching for the equilibrium structure and then calculated the density of states (DOS) of the unit layer of our Ru complex. Here we adopt the spin-polarized density functional theory (DFT). The unit cell structure is given in the inset of Figure 5. The molecule is slightly twisted along the C_2 axis, which is defined as the vector parallel to the normal line direction of the layer film. The resulting DOS is also shown in Figure 5, where it may be readily noticed that the DOS has a clear peak at the Fermi level of the molecular layer. It should be noticed that the DOS is not spiky thanks to two-dimensional periodicity: we are discussing a molecular layer, not an isolated molecule. For comparison, the DOS of the vacancy system, which is obtained by replacing the two Ru atoms with vacancies, is also included in the figure. At the Fermi level, the vacancy system has a clear energy gap. Figure 7 reveals that a Ru-originated band is formed in our complex SAM that is partially filled. This means that there is an effective transfer integral between two adjacent Ru atoms despite the large distance between them. Later we will show that the effective transfer integral plays an important role in the stepping-stone mechanism.

Next we discuss contact between the Ru complex and electrodes to investigate the possibility of contact asymmetry. We made some simplifications for electrodes and the Ru complex layer. First, Au(001) is used instead of ITO as electrodes. Multileg phosphoric acid anchors are simplified to single-leg thiol anchors to prevent too much demand on computational resources. A phenyl ring was omitted for the same reason. The resulting geometry is depicted in Figure 6. The present model system preserves the most important features of our Ru complex; that is, the Ru centers form a narrow band and the C_2 symmetry is broken by twisting. We thus believe that the present simplification is valid for checking the presence of contact asymmetry. Note that this model compound is also a good approximation for other metal complexes.[11]

We calculated the projected molecular orbitals (PMOs)[34] onto the model Ru complex region using the entire single-body Hamiltonian, including electrodes. This Hamiltonian is constructed from self-consistent molecular orbitals. The four PMOs, whose energies are close to E_F of the gold electrode, are plotted in Figure 6. Only LUMOs (a), (b), and (d) have amplitudes on anchoring S atoms. This localization of the PMOs on each Ru-center moiety is caused by broken symmetry due to the twisted structure. Furthermore, the spin polarization, *i.e.*, the difference between up and down spin distribution, enhances the difference of MOs for major and minor spin. This could enhance the spatial asymmetric distribution of the wave functions. The details of the localization of PMOs will be analyzed elsewhere (unpublished work).

Using the self-energy formalism, the coupling strength of each PMO with the left (right) electrodes, which relate to Γ_L (Γ_R) at E_F, was estimated.[34] We found a sufficiently large contact asymmetry for all the calculated PMOs. The ratio Γ_L/Γ_R is estimated to be 0.0, 0.33, and 970 for LUMOs (a), (b), and (d). The long-range effective transfer integral and the contact asymmetry characterize the Ru complex system. These features need to be taken into account in the tight binding model we are going to build. We are aware that our model anchor used in our first-principles calculations may be too simplified to describe the real anchoring group; that is, a possibly stronger potential barrier effect at the phosphoric acid anchor may provide a largely different chemical setup. Nonetheless, we still believe that our points above are important for discussing the physics of our problem. This is because of a mathematical constraint on the transmission probability. If the contacts were symmetric, a low but long-range charge migration rate would not be possible; that is, a small β value necessarily leads to a high conductance value. This mathematical requirement exerts a stronger constraint on the transport property than the chemical setup. This will be discussed further in the subsequent section.

Stepping-Stone Mechanism. As stated in the First-Principles Calculations section, Ru atoms play a major role in charge migration across the insulating carbon backbone. Hence, we need some extensions introducing

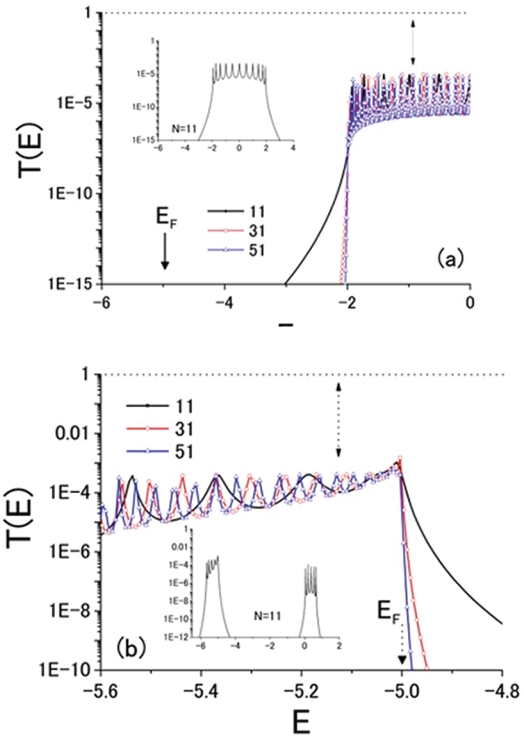

Figure 8. Transmission coefficients $T(E)$ of (a) hydrocarbon chains and (b) the Ru complex chain represented by the parameter set (i) and (ii). Only in the latter case do we observe that the probability $T(E)$ does not decay exponentially as we increase the chain length from $N = 11$ to $N = 31$ and 51. The numbers in the legend denote the number of sites in the chain. See the text for more information.

inhomogeneity into the model used in the previous study. The simplest extension to the molecular part of the Hamiltonian would be obtained by introducing *heterogeneous site potentials* into the model:

$$H_{\mathrm{mol}} = \sum_i \varepsilon_i^a n_i^a + \sum_i \varepsilon_i^b n_i^b - t \sum_{\langle i,j\rangle,\sigma} (a_{i\sigma}^\dagger b_{j\sigma} + b_{j\sigma}^\dagger a_{i\sigma})$$

where n_i^a and n_i^b denote $a_{i\uparrow}^\dagger a_{i\uparrow} + a_{i\downarrow}^\dagger a_{i\downarrow}$ and $b_{i\uparrow}^\dagger b_{i\uparrow} + b_{i\downarrow}^\dagger b_{i\downarrow}$, respectively, and σ denotes spins $\uparrow$ and $\downarrow$. $\varepsilon^{a(b)}$ and t denote $a(b)$ site energy and the transfer integral (half-"bandwidth" in our case). $\langle\rangle$ in the last summation means that the transfer is limited to nearest neighbors. The electrode (donor/acceptor) part and the coupling between the molecule and the electrode (donor/acceptor) were accounted for in terms of the same formalism as described in ref 7. The contact asymmetry was taken into account by using different values for transfer integrals t_L and t_R between the Ru complex and the left and right electrodes, respectively.

Site "*a*" may represent a frontier molecular orbital of the bridging phenyl ring at the center of the complex and/or 2,6-bis(benzimidazol-2-yl)pyridine with a phosphonate group, which makes a contribution to the second lowest peak of the DOS above E_F in Figure 5. Site "*b*" may represent a frontier molecular orbital of the bis(tridentate ligand) ruthenium(II) derivative centered on the 4d and 5s atomic orbitals of the Ru atom, which contributes to the lowest peak of the DOS above E_F. Note that the ionization potential (I_P) of the Ru atom is much greater than the work function of bulk Au, and the LUMO energy of the tris-bipyridine moiety will be sufficiently higher than E_F. It is therefore reasonable to suppose that hybridization of the Ru and bis-(tridentate) ligand orbitals may provide a frontier orbital close in energy to E_F. We therefore assume that site "*a*" is higher in energy than site "*b*". Sites "*a*" and "*b*" are linearly aligned: ... *ababab* .... I_P of the conjugated molecular moiety may be significantly different from that of the metal atom, and therefore we may expect $|(\varepsilon^a - \varepsilon^b)/t| \gg 1$. Assuming this limit, the direct transfer of electrons between two adjacent "*a*" sites and two adjacent "*b*" sites may arise, both with the small *effective* transfer integral $\tilde{t} = t^2/|(\varepsilon^a - \varepsilon^b)|$. We would therefore expect a density of states formation with a narrow bandwidth of $2\tilde{t}$ around ε^a and ε^b. This argument is based on second-order perturbation theory and is depicted in Figure 8. The Ru-originated narrow band formation thus obtained does not contradict our first-principle results.

The emergence of density of state around ε^a and ε^b is also found in the transmission coefficient $T(E)$ represented in Figure 8. We have plotted the energy E dependence of the transmission probabilities for the two cases (i) $\varepsilon^a = \varepsilon^b = 0$ (representing alkanes and conjugated hydrocarbon chains) and (ii) $\varepsilon^a = 0, \varepsilon^b = -5t$ (representing the Ru complex chains). In both cases, we used a three-dimensional cubic lattice model for the left and right electrodes. We then placed the transfer integral and the site energy there using $t_M = -10t$ and $\varepsilon_M = -5t$, respectively. The link transfer integrals between the molecule and the left and the right electrodes are given by $t_L = t_R = t$, and hence $t_R/t_L = 1$ in the case of symmetric contact, but $t_L = t$, $t_R = 0.01t$ and hence $t_R/t_L = 0.01$ for asymmetric contact. Details of the contact self-energy and these parameters are described in ref 7. When we set the Fermi level E_F and/or donor−acceptor level to $-5t$, the site "*b*" energy is *resonant* with E_F and/or E_{DA} for (ii), but is far from resonance for (i). The transmission coefficients of some chains with different lengths $L = Nd$, where d denotes the intersite distance and N is the number of moieties, are given in Figure 7. $T(E_F)$ and/or $T(E_{DA})$ clearly decays exponentially in (i), but remains virtually constant (oscillates when a small energy mismatch is expected) as a function of N. We have checked that the elongation of the alignment period with varieties such as ... *abbabbabb* ... and ... *aabaabaab* ... does not change the essential results, but the energy region where $\beta = 0$ is satisfied narrows. These results suggest that our Ru complex layers might exhibit long-range charge migration with a decay constant of $\beta = 0$. Long-range transport could then be realized mainly through small direct effective transfer between adjacent Ru (4d) orbitals mediated by the large potential barrier at the

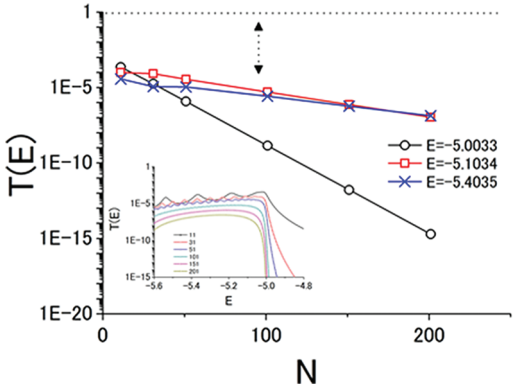

Figure 9. Dephasing effect on the length dependence of the transmission probability of the Ru complex chain. The dephasing term κ mimics the electron−phonon scattering effect. The dephasing effect causes damped oscillation in the energy region, where a simple oscillation is otherwise expected. The exponent γ of the length dependence represented in the form of $e^{-\gamma N}$ is roughly estimated to be $\gamma = 0.03$ when $\kappa = 0.01t$.

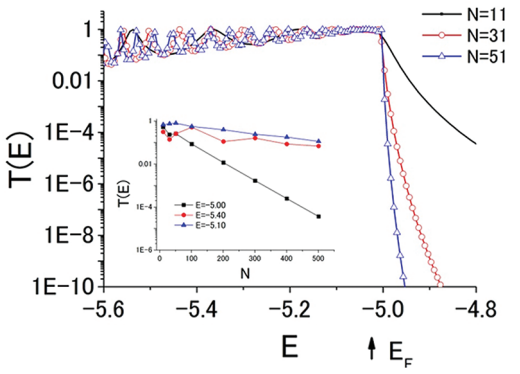

Figure 10. Transmission coefficient $T(E)$ for the symmetric contact case, *i.e.*, $t_R/t_L = 1$. Other parameter values are the same as those used to obtain Figures 8b and Figure 9; we used the parameter set (ii). The length dependence at some energies is shown in the inset. The exponent $T(E)$ is estimated to be 0.003 (at $E = -5.1t$) in this case. These small exponent values are obtained only when $T(E)$ is high in the case of symmetric contact.

carbon (cage) backbone in the center of the Ru complex and/or 2,6-bis(benzimidazol-2-yl)pyridine with the phosphonate group. The network of Ru centers acts as "stepping-stones", bridging electrodes across off-resonant potential sites. Long-range tunneling is thus distinct from the standard resonant tunneling described by homogeneous tight binding sites. This is why we call it a "*stepping-stone mechanism*".

Although the stepping-stones provide a mediated resonant tunneling mechanism, $T(E_F)$ can be much smaller than 1 when $t_R/t_L \gg 1$ or $t_R/t_L \ll 1$, and hence $\Gamma_R/\Gamma_L \gg 1$ or $\Gamma_R/\Gamma_L \ll 1$. $T(E_F)$ may always reach 1 at some length L when $t_R/t_L = 1$. Numerically, it is very difficult to reach the value of 1, and we only come close to the value, because of the extreme sharpness of the peaks. The transmission coefficient is much reduced by the contact asymmetry. The magnitude of the reduction depends largely on the asymmetry ratio. Hence, our mechanism, *i.e.*, a combination of stepping-stone and contact asymmetry, explains the long-range, but low-charge migration rate that is observed experimentally in our Ru complex system.

The last problem is the origin of the finite but nonzero exponent in the stepping-stone mechanism. One possible reason is slight energy mismatching of the "stepping-stone" site due to the multiband effect since the metal center can provide quasi-degenerate orbitals. As another possibility, the dephasing effect would be important, particularly if the length increases. Figure 9 shows the length dependence of $T(E_F)$ where the parameter set (ii) used is augmented with the additional dephasing term $\kappa = 0.01t$. As it is found in the (single-band) tight binding model based on the homogeneous sites[7] and described in the previous section, the dephasing term brings about damped oscillation with small exponent γ, which is estimated to be 0.03 when $E = -5.4t$. This may correspond to $\gamma_d = 0.002$ Å^{-1}, where the length dependence is described in terms of L but not of N, assuming that the intersite distance can be estimated by $d = 15$ Å. This result indicates that the length-independent ($\beta = 0$) tunneling shown in Figure 10b is very easily modified to damped oscillation with a finite exponent value. This is because the bandwidth of our resonant state $2\tilde{t}$ is so narrow that it is very sensitive to perturbations such as vibronic couplings. The extremely sharp peaks given in Figure 8 are unable to resist even the smallest perturbations. In short, competition between the stepping-stone mechanism and vibronic interactions leads to the observed slow but non-negligible exponential decay of charge migration rate in our Ru complex.

To indicate how important contact symmetry is for our problem, the corresponding plots in Figures 8b and 9 are shown in Figure 10, where the same parameter values that give these results, but with different symmetry of the contacts, were used. This result, along with Figure 9 in ref 7, means that contact asymmetry is crucial to realizing a low but long-range conductance and/or charge migration rate. While the chemical model used in our first-principles calculation may have some problems in light of the chemical reality of our experimental system, the general conclusion, indicating the importance of asymmetric contact, has a robust mathematical reasoning. A possible higher barrier height of the phosphoric acid anchor than thiol may be represented by an increase in the site energy gap, *i.e.*, $\varepsilon^a - \varepsilon^b$. This will make the width of the narrow band $|2t'| = |2t^2/(\varepsilon^a - \varepsilon^b)|$ even narrower. Bandwidth narrowing is what we expect from the possible barrier height increase in the anchoring site. This will lead to a sharpening, rather than a reduction, of the transmission peak.

CONCLUSIONS

We studied the thickness dependence of the charge migration rate and/or electric current through Ru complex multilayer films. The multilayer films were prepared *via* a spontaneous growth technique using pH-dependent aggregation of hydrogen bonds. The molecular unit structure of our Ru complex multilayer films resembles that of redox-active Co/Fe complexes, which have been reported to show long-range charge migration ability.[11,13] We made a cross-check of the results obtained using the electrochemical method and the sandwiched solid cell measuring electron transfer rate and electric current, respectively. The latter was done with special attention paid to reducing the pinhole effect using PEDOT:PSS as electrodes. We observed small β values of 0.012−0.021 Å^{-1}, indicating that our Ru complex multilayer exhibits long-range electron transport ability. We have experimentally estimated the activation energy to be as small as 10−16 meV, suggesting a tunneling mechanism.

A possible mechanism for the small β value was investigated by focusing on the key role of metal centers. On the basis of the results of theoretical−experimental collaboration, we propose a modified tunneling mechanism, which we named the "stepping-stone mechanism". The existence of the lower bound β_{LB} (= 2 log 2) of the exponent for standard off-resonant tunneling places strong constraints on the mechanism of the small β value. If the exponential decay of conductance or charge transfer rate is slower than $e^{-\beta_{LB}N}$, a novel mechanism other than the standard one may be necessary. A rough estimate gives us the critical value of $\beta_{LB} = 0.1$ Å^{-1} for the Ru complex, since the intersite distance there may be about ∼15 Å. Thus, the conventional tunneling mechanism is very unlikely in our case. We propose a mechanism for the small β value in terms of a stepping-stone-like alignment of atomic potentials around the Fermi level. Our stepping-stone mechanism may be one of the most realistic possibilities and appears to support the intuitive arguments made in the literature.[11−13] Vibronic coupling may be necessary to explain the small but nonzero exponent. Contact asymmetry is another important contributor to explaining the low charge migration rate.

Our state-of-the-art theoretical result is distinct from previous arguments made almost 20 years ago[8−10] on the mechanism of the small β value, which mostly depend on randomness and the presence of pinholes. Justifying the latter in the new class of organometallic layers may have to be rigorously tested, since it is not as yet convincingly supported at the microscopic level. First-principles calculations are now in progress on the length dependence of ballistic conductance for several kinds of metal-center complex layers. The usefulness of organometallic-complex molecular layers for molecular devices has not yet been utilized in any way. Their potential should be examined in the near future.

METHODS

Immobilization of the Ru Complex. Atomically flat ITO-coated glass (purchased from Kuramoto Co. with sheet resistance <10 Ω/sq) was used as the substrate. The molecular film of the Ru complex with eight anchoring phosphonic acids as shown in Figure 1 is fabricated onto the ITO-coated glass. The ITO substrates were cleaned by sonication in acetone for 5 min and thoroughly rinsed with acetone. To immobilize the Ru complex, the precleaned ITO substrate was then immersed in a 25 μM mixture solution (MeOH−H_2O = 1:1 v/v) of the Ru complex adjusted to pH 3 or pH 6. The pH value of the solution was fine-tuned by adding small amounts of 0.1 M KOH(aq) or 0.1 M HCl(aq) to the above MeOH+H_2O solution mixture containing the Ru complex. After immobilization of the Ru complex, the ITO substrate was washed with MeOH−H_2O (= 1:1 v/v) mixed solution to remove any weakly adsorbed molecules and contaminants.

XPS, FT-IR, and AFM Measurements. XPS spectra were measured using a Theta Probe system from Thermo VG Scientific Inc. using a focused monochromatic Al Kα X-ray source (1486.6 eV). In the present study, the binding energy was calibrated using the C(1s) binding energy of 284.8 eV for contaminated carbon species on the bare ITO surface. The X-ray power, spot size, and pass energy of the analyzer were set at 45 W (15 kV, 3 mA), 200 μm, and 50 eV. The thickness of the Ru complex layer immobilized on ITO can be estimated using the equation[17]

$$d = -\lambda \cos\theta \ln(I/I_0)$$

where d is the film thickness, I_0 and I are the In(3d) intensity before and after film formation, λ is the attenuation length of the In(3d) electron from the ITO surface, and θ is the takeoff angle from the surface normal. In the present study, we measured the spectrum at $\theta = 0°$. We used a wavelength of 3.5 nm to determine the thickness of the Ru complex layer.[17] FT-IR −RAS spectra were taken using the Magna-760 system (Thermo Nicolet) at 4 cm^{-1} resolution. AFM images were obtained using a Seiko Instruments SPA400 unit in dynamic force mode. We used a 20 N/m silicon cantilever whose tip radius was approximately 20 nm.

Electrochemical Measurements. Electrochemical measurements of the Ru(II) complex-modified ITO surfaces as a working electrode were carried out on a conventional three-electrode cell with an ALS/CH Instruments model 611 C electrochemical analyzer at 25 °C in 0.1 M tetrabutyl ammonium perchlorate (TBAP) in CH_3CN solution. The auxiliary and reference electrodes were platinum wire and Ag/$AgNO_3$ (0.01 M $AgNO_3$), respectively. To estimate the electron transfer kinetic constant, chronoampermetry measurements were performed in potential steps from +0.40 V to +1.17 V *versus* Ag/Ag$^+$ to the crossover redox potential (at around +0.70 V vs Ag/Ag$^+$) of Ru complex layers.[13,16,19] Before the electrochemical measurements, the setup was purged with pure nitrogen gas for 20 min to remove any dissolved oxygen in the solution.

Sandwich Cell Fabrication and *I*−*V* Measurements. Solid-state sandwich cells of poly(3,4-ethylenedioxythiophene) stabilized with poly(4-styrenesulfonic acids) (hereafter PEDOT:PSS)|Ru complex layer|ITO junction (*cf.* Figure 4a) are fabricated as follows.[27−29] Before formation of the Ru complex layer onto the ITO surface, a polycrystalline insulating TiO_2 layer (∼100 nm) was sputter-deposited onto an unheated metal mask covering the ITO substrate using a rf magnetron

(KS-702KAM-AI2 K-science-inc., Japan). The base pressure in the sputtering chamber was less than 10^{-4} Pa. Sputter deposition was carried out in a mixture of Ar and O_2 (5%) gas at room temperature. Before deposition, the surface of the target was cleaned for 2 min at 200 W. The deposition rate was set at 20 nm/min (rf power 125 W). After two 50 nm depositions, to change the amorphous TiO_2 film on ITO into polycrystalline film, the film was annealed at 350 °C for 1 h in air. Even under the metal mask, small TiO_2 particles remain, so the substrate was washed in KOH for 2 min to remove them. The Ru complex layer immobilization was carried out as previously described. PEDOT:PSS was then coated on the Ru complex layer. To increase the conduction of the PEDOT:PSS film, 5 wt % ethylene glycol was added to the PEDOT:PSS liquid.[30] To remove the water in the PEDOT:PSS, the substrate was annealed at 60 °C for 10 min in air. The obtained thickness of PEDOT:PSS was 4 μm, estimated using SEM imaging. Current–voltage measurements were carried out using the 4200-SCS system (Keithley Instruments, Inc.). In particular samples, to obtain the temperature dependence of the $I-V$ curves, sandwich cells were cooled using liquid N_2 in a vacuum system.

Computational Methods. The electronic structure calculations were performed in terms of density functional theory using the SIESTA package.[35] The Perdew–Burke–Ernzerhof exchange correlation functional and the pseudo atomic orbital type basis set were used.[36] We adopted a split-valence double-ζ with polarization for H, C, N, S, and Ru atoms and a single-ζ with polarization for the Au electrodes. For calculations of the equilibrium structure and the DOS of our Ru complex, we took a unit cell with periodic boundary condition, with cell vectors large enough to neglect interactions between neighboring Ru complexes. The resulting DOS was then smeared due to the two-dimensional periodicity. To carry out the PMO analysis and calculate molecule–electrode coupling strength of the model Ru complex contact, the nonequilibrium Green's function technique[37] was applied. The first-principles calculations of the Green's function, $G(E)$, and left/right self-energy terms, $\Sigma_{L/R}(E)$, were performed using the HiRUNE module program.[38] We took the Au(001) surface as electrodes and included five layers for each side electrode in the Green's function calculations. Two-dimensional periodic boundary conditions are imposed for a surface with a $c(5\times5)$ unit cell. Monkhorst–Pack 3×3 was adopted for k-point sampling, while the PMOs were defined on the Γ point. Note that we also optimized the structure of model contact by relaxing only the atoms in the model Ru complex. The distance between the electrodes was fixed at 27.93 Å. Using the terms $G(E)$, $\Sigma_L(E)$, and $\Sigma_R(E)$, the self-energies were renormalized onto the molecular projected state Hamiltonian. The $\Gamma_{L/R}$ couplings were then obtained for each PMO.

Conflict of Interest: The authors declare no competing financial interest.

Acknowledgment. We would like to thank S. Sasaki and H. Ogawa at Tokyo University of Science for their helpful suggestions and assistance with the experiment. We would like to thank the Ministry of Education, Culture, Sports, Science and Technology (MEXT) for the Grant-in-Aid for Scientific Research for Priority Area (No. 20111015) "Emergent chemistry of nanoscale molecular systems", to T.I., for Priority Area (No. 21108003) "Coordination Programming" for a Grant-in-Aid for Scientific Research (No. 21350082) to M.H., and for Grant-in-Aid for Scientific Research (C) #20613002 to H.N. H.N and Y.A are also grateful to the financial support by the Scientific Research on Innovative Areas, a MEXT Grant-in-Aid Project: "Materials Design through Computics" (#23104514). We would also like to thank M. Nakano, K. Miyake, Y. Naitoh, M. Horikawa, and H. Suga of AIST for their support with XPS and $I-V$ measurements.

Supporting Information Available: FT-IR spectra (Figure S1), AFM images of Ru complex layers (Figure S2), cyclic voltammograms (CV) of modified ITO substrate with Ru complex layers (Figure S3), and temperature dependence of the current though Ru complex layers (Figure S4). This material is available free of charge *via* the Internet at http://pubs.acs.org.

REFERENCES AND NOTES

1. Aviram, A.; Ratner, M. A. *Molecular Electronics: Science and Technology*; Academy of Sciences: New York, 1998.
2. May, V.; Kuhn, O. *Charge and Energy Transfer Dynamics in Molecular Systems*; Wiley-VCH: Berlin, 2000.
3. Mujica, V.; Kemp, M.; Ratner, M. A. Electron Conduction in Molecular Wires. 1. A Scattering Formalism. *J. Chem. Phys.* **1994**, *101*, 6849–6855.
4. Mujica, V.; Kemp, M.; Ratner, M. A. Electron Conduction in Molecular Wires. 2. Application to Scanning Tunneling Microscopy. *J. Chem. Phys.* **1994**, *101*, 6856–6864.
5. Ie, Y.; Hirose, T.; Nakamura, H.; Kiguchi, M.; Takagi, N.; Kawai, M.; Aso, Y. Nature of Electron Transport by Pyridine-Based Tripodal Anchors: Potential for Robust and Conductive Single-Molecule Junctions with Gold Electrodes. *J. Am. Chem. Soc.* **2011**, *133*, 3014–3022.
6. Patrone, L.; Palacin, S.; Bourgoin, J. P. Direct Comparison of the Electronic Coupling Efficiency of Sulfur and Selenium Alligator Clips for Molecules Adsorbed onto Gold Electrodes. *Appl. Surf. Sci.* **2003**, *212*, 446–451.
7. Asai, Y.; Fukuyama, H. Theory of Length-Dependent Conductance in One-Dimensional Chains. *Phys. Rev. B* **2005**, *72*, 085431.
8. Hong, H. G.; Mallouk, T. E. Electrochemical Measurements of Electron-Transfer Rates through Zirconium 1,2-Ethanediylbis(phosphonate) Multilayer Films on Gold Electrodes. *Langmuir* **1991**, *7*, 2362–2369.
9. Hong, H. G.; Sackett, D. D.; Mallouk, T. E. Adsorption of Well-Ordered Zirconium Phosphonate Multilayer Films on High Surface-Area Silica. *Chem. Mater.* **1991**, *3*, 521–527.
10. Finklea, H. O.; Avery, S.; Lynch, M.; Furtsch, T. Blocking Oriented Monolayers of Alkyl Mercaptans on Gold Electrodes. *Langmuir* **1987**, *3*, 409–413.
11. Tuccitto, N.; Ferri, V.; Cavazzini, M.; Quici, S.; Zhavnerko, G.; Licciardello, A.; Rampi, M. A. Highly Conductive Approximately 40-nm-Long Molecular Wires Assembled by Stepwise Incorporation of Metal Centres. *Nat. Mat.* **2009**, *8*, 41–46.
12. McCreery, R. L. Electron Transport and Redox Reactions in Molecular Electronic Junctions. *ChemPhysChem* **2009**, *10*, 2387–2391.
13. Nishimori, Y.; Kanaizuka, K.; Kurita, T.; Nagatsu, T.; Segawa, Y.; Toshimitsu, F.; Muratsugu, S.; Utsuno, M.; Kume, S.; Murata, M.; *et al.* Superior Electron Transport Ability of π-Conjugated Redox Molecular Wires Prepared by the Stepwise Coordination Method on a Surface. *Chem. Asian J.* **2009**, *4*, 1361–1367.
14. Haga, M.; Kobayashi, K.; Terada, K. Fabrication and Functions of Surface Nanomaterials Based on Multilayered or Nanoarrayed Assembly of Metal Complexes. *Coord. Chem. Rev.* **2007**, *251*, 2688–2701.
15. Ishida, T.; Terada, K.; Hasegawa, K.; Kuwahata, H.; Kusama, K.; Sato, R.; Nakano, M.; Naitoh, Y.; Haga, M. Self-Assembled Monolayer and Multilayer Formation using Redox-Active Ru Complex with Phosphonic Acids on Silicon Oxide Surface. *Appl. Surf. Sci.* **2009**, *255*, 8824–8830.
16. Motiei, L.; Lahav, M.; Gulino, A.; Iron, M. A.; van der Boom, M. E. Electrochemical Characteristics of a Self-Propagating Molecular-Based Assembly. *J. Phys. Chem. B* **2010**, *114*, 14283–14286.
17. Schlapak, R.; Armitage, D.; Saucedo-Zeni, N.; Hohage, M.; Howorka, S. Preparation and Characterization of Dense Films of Poly(amidoamine) Dendrimers on Indium Tin Oxide. *Langmuir* **2007**, *23*, 8916–8924.
18. Rusu, C. N.; Yates, J. T., Jr. Adsorption and Decomposition of Dimethyl Methylphosphonate on TiO_2. *J. Phys. Chem. B* **2000**, *104*, 12292–12298.
19. Kurita, T.; Nishimori, Y.; Toshimitsu, F.; Muratsugu, S.; Kume, S.; Nishihara, H. Surface Junction Effects on the Electron Conduction of Molecular Wires. *J. Am. Chem. Soc.* **2010**, *132*, 4524–4525.

20. Bumm, L. A.; Arnold, J. J.; Dunbar, T. D.; Allara, D. L.; Weiss, P. S. Electron Transfer through Organic Molecules. *J. Phys. Chem. B* **1999**, *103*, 8122–8127.
21. Wold, D. J.; Frisbie, C. D. Formation of Metal−Molecule−Metal Tunnel Junctions:Microcontacts to Alkanethiol Monolayers with a Conducting AFM Tip. *J. Am. Chem. Soc.* **2000**, *122*, 2970–2971.
22. Cui, X. D.; Primak, A.; Zarate, X.; Tomfohr, J.; Sankey, O. F.; Moore, A. L.; Moore, T. A.; Gust, D.; Harris, G.; Lindsay, S. M. *Reproducible Meas. Single-Mol. Conductivity Sci.* **2001**, *294*, 571–574.
23. Ishida, T.; Mizutani, W.; Aya, Y.; Ogiso, H.; Sasaki, S.; Tokumoto, H. Electrical Conduction of Conjugated Molecular SAMs Studied by Conductive Atomic Force Microscopy. *J. Phys. Chem. B* **2002**, *106*, 5886–5892.
24. Luo, L.; Frisbie, C. D. Length-Dependent Conductance of Conjugated Molecular Wires Synthesized by Stepwise "Click" Chemistry. *J. Am. Chem. Soc.* **2010**, *134*, 8854–8855.
25. Holmlin, R. E.; Haag, R.; Chabinyc, M. L.; Ismagilov, R. F.; Cohen, A. E.; Terfort, A.; Rampi, M. A.; Whitesides, G. M. Electron Transport through Thin Organic Films in Metal−Insulator−Metal Junctions Based on Self-Assembled Monolayers. *J. Am. Chem. Soc.* **2001**, *123*, 5075–5085.
26. Anariba, F.; McCreery, R. L. Electronic Conductance Behavior of Carbon-Based Molecular Junctions with Conjugated Structures. *J. Phys. Chem. B* **2002**, *106*, 10355–10362.
27. Akkerman, H. B.; Blom, P. W. M.; de Leeuw, D. M.; de Boer, B. Towards Molecular Electronics with Large-Area Molecular Junctions. *Nature* **2006**, *441*, 69–72.
28. Akkerman, H. B.; de Boer, B. Electrical Conduction through Single Molecules and Self-Assembled Monolayers. *J. Phys.: Condens. Matter* **2008**, *20*, 013001.
29. Akkerman, H. B.; Kronemeijer, A. J.; Harkema, J.; Hal, P. A.; van; Smits, E. C. P.; de Leeuw, D. M.; Blom, P. W. M. Stability of Large-Area Molecular Junctions. *Org. Electron.* **2010**, *11*, 146–149.
30. Dimitriev, O. P.; Grinko, D. A.; Noskovb, Yu. V.; Ogurtsov, N. A.; Pud, A. A. PEDOT:PSS Films-Effect of Organic Solvent Additives and Annealing on the Film Conductivity. *Synth. Met.* **2009**, *159*, 2237–2239.
31. Datta, S. *Electronic Transport in Mesoscopic Systems*; Cambridge University Press: Cambridge, 1995.
32. Asai, Y. Theory of Electric Conductance of DNA Molecule. *J. Phys. Chem. B* **2003**, *107*, 4647–4652.
33. Datta, S. *Quantum Transport: Atom to Transistor*; Cambridge University Press: Cambridge, 2005.
34. Nakamura, H.; Asai, Y.; Hihath, J.; Bruot, C.; Tao, N. J. Switch of Conducting Orbital by Bias-Induced Electronic Contact Asymmetry in a Bipyrimidinyl-biphenyl Diblock Molecule: Mechanism to Achieve a *pn* Directional Molecular Diode. *J. Phys. Chem. C* **2011**, *115*, 19931–19938.
35. Soler, J. M.; Artacho, E.; Gale, J. D.; Garcia, A.; Junquera, J.; Ordejon, P.; Sanchez-Portal, D. The SIESTA Method for *ab initio* Order-N Materials Simulation. *J. Phys.-Condens. Matter* **2002**, *14*, 2745–2779.
36. Junquera, J.; Paz, O.; Sanchez-Portal, D.; Artacho, E. Numerical Atomic Orbitals for Linear-Scaling Calculations. *Phys. Rev. B* **2001**, *64*, 235111.
37. Stokbro, K.; Taylor, J.; Brandbyge, M.; Mozos, J. L.; Ordejon, P. Theoretical Study of the Nonlinear Conductance of Dithiol Benzene Coupled to Au(111) Surfaces via Thiol and Thiolate Bonds. *Comput. Mater. Sci.* **2003**, *27*, 151–160.
38. Nakamura, H.; Yamashita, K. An Efficient Molecular Orbital Approach for Self-Consistent Calculations of Molecular Junctions. *J. Chem. Phys.* **2006**, *125*, 194106.